IEEE Transactions on Nuclear Science, Vol.NS-22, No.3, 1975

TUNE SHIFTS OF EXCENTRIC BEAMS IN ELLIPTIC VACUUM CHAMBERS

B.W. Zotter
CERN
Geneva, Switzerland

Introduction

High-energy particle accelerators and storage ings require a close control of the betatron tune in rder to avoid beam blow-up and particle loss by noninear resonances. For this reason, one needs a good nowledge of the tune shifts caused by space-charge orces. These are conventionally separated into one ontribution due to the "direct" space-charge force, hich remains unchanged when the chamber walls are reoved, and one due to "image" effects caused by the resence of surrounding walls, and which usually domiate at higher energies.

We further have to distinguish between the coherent" tune-shift, which expresses the change of he betatron frequency when the beam oscillates as a hole (not included here because of space limitations), nd the "incoherent" shift which changes the single article tune. It has become customary to express the mage tune shifts as the product of a factor containing he beam parameters, and a factor that consists essenially of the sum of geometric coefficients divided by he squares of appropriate chamber dimensions.

Ordinary non-magnetic, metallic vacuum chamber alls cause only an electric image force for coasting eams, while a magnetic image is formed by the poleieces of the magnets surrounding the chamber. For unched beams, however, also the magnetic image is ormed by the chamber walls, and a strong cancellation f the image forces results.

These "image-coefficients" are proportional to deivatives of the forces acting on the beam. In general, e need to know them in two orthogonal directions - sually taken as horizontal and vertical. Outside the eam proper, the incoherent image coefficients obey aplace's equation, and hence are of equal magnitude ut opposite sign. This does not hold for the coherent mage coefficients, however, which contain the derivaive of the field with respect to the source co-ordinate, nd which therefore have to be calculated in both planes.

Image Coefficients in a Circular Chamber

Before we discuss the more complicated case of lliptic chambers, we derive the relevant expressions or circular ones. A line charge λ, situated on the orizontal axis at x_1, has a single image of opposite harge at

$$x_2 = \frac{R^2}{x_1} \tag{1.1}$$

here R is the chamber radius. The potential along the -axis is then given by

$$U = -\frac{\lambda}{2\pi\varepsilon_0}\ln\left|\frac{x-x_1}{x-x_2}\right| \tag{1.2}$$

nd the horizontal component of the electric field ecomes

$$E_x = -\frac{\partial U}{\partial x} = \frac{\lambda}{2\pi\varepsilon_0}\left[\frac{1}{x-x_1}+\frac{1}{x-x_2}\right] \tag{1.3}$$

The first term in brackets is the direct space-charge term, which remains unchanged when the walls are removed to infinity. From the second term, we obtain the incoherent image coefficients

$$\varepsilon_1{}^h(x,x_1) = -\,\varepsilon_1{}^v(x,x_1) = \frac{\pi\,\varepsilon_0\,R^2}{\lambda}\,\frac{\partial E_x^{IM}}{\partial x} \tag{1.4}$$

or, using the normalized variables

$$\eta \equiv \frac{x}{R}, \qquad \eta_1 \equiv \frac{x_1}{R} \tag{1.5}$$

$$\varepsilon_1{}^h(\eta,\eta_1) = -\,\varepsilon_1{}^v(\eta,\eta_1) = \frac{\eta_1{}^2}{2(1-\eta\eta_1)^2} \tag{1.6}$$

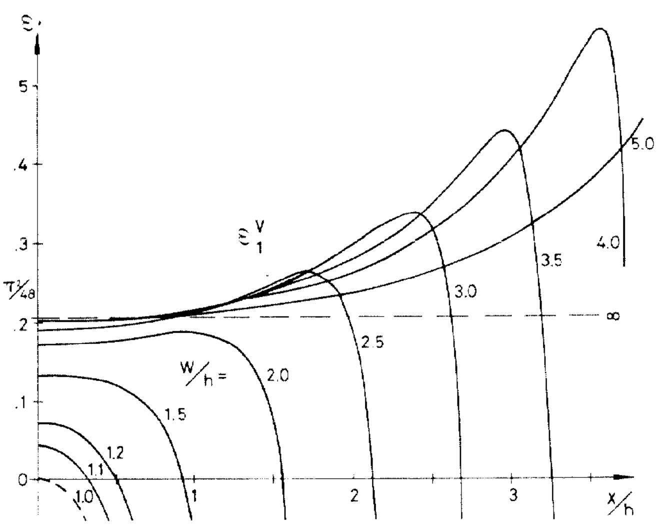

Fig. 1 - Incoherent image coefficient of thin beams on the major axis of elliptical vacuum chambers, for varying aspect ratios w/h, as function of the distance from the centre x/h.

The image coefficients at the beam location are found for $\eta = \eta_1$. They are shown in Fig. 1, together with the coefficients of elliptic chambers. It can be seen that $\varepsilon_1 = 0$ at the centre of a circular chamber, but reaches values above the coefficient of the parallel-plate geometry ($\pi^2/48$) already half way to the wall. However, as their signs are opposite, the contributions due to circular and due to elliptic chambers (or flat pole pieces) tend to cancel to some degree. This will no longer be true, however, for superconducting machines with purely circular chambers and iron surfaces.

The image coefficient of a beam of finite half-width a - but negligible height - centred at x_c can be found from the integral

$$\varepsilon_1(x;x_0,a) = \frac{1}{2a}\int_{x_0-a}^{x_c+a} \varepsilon_1(x,x_1)\,dx_1 \tag{1.7}$$

for beams of uniform density. The integral is readily evaluated and yields (with $\alpha = a/R$) (1.8)

$$\varepsilon_1{}^h(\eta;\eta_o,\alpha) = \frac{1}{2\eta^2}\left[1 + \frac{1}{u^2 - v^2} + \frac{1}{v}\ln\frac{u - v}{u + v}\right] \quad (1.9)$$

where

$$u = 1 - \eta\eta_o \qquad v = \alpha\eta \quad (1.10)$$

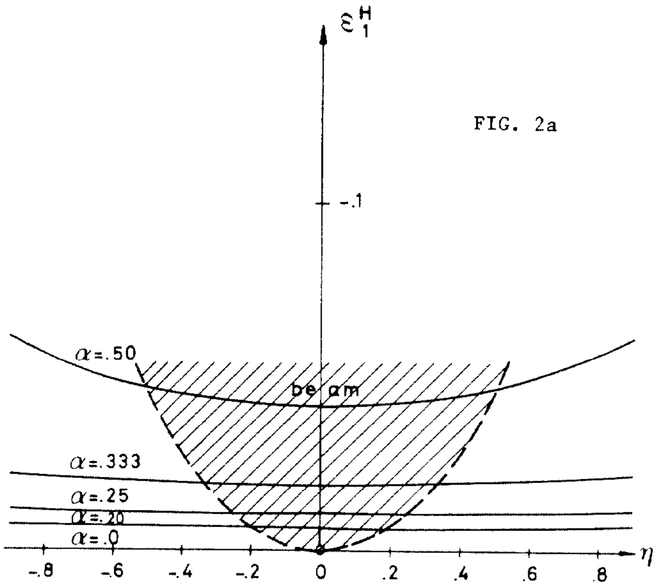

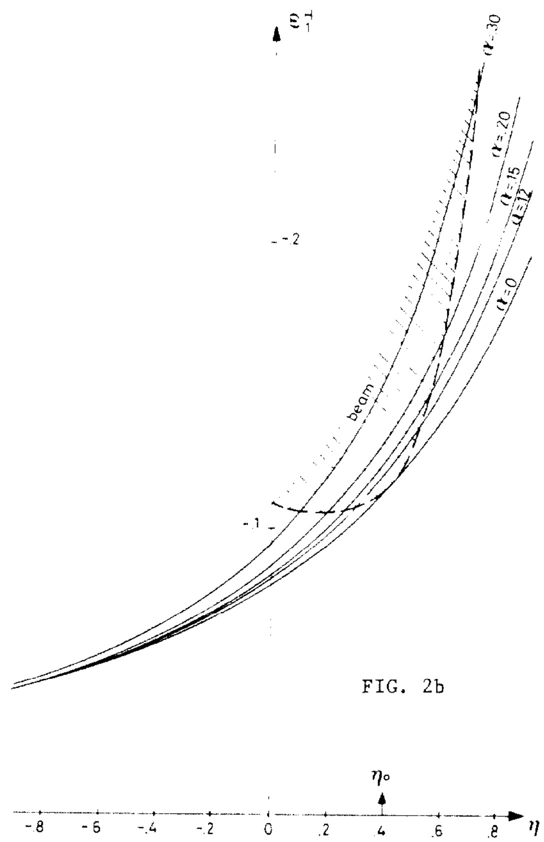

Fig. 2 - Incoherent image coefficients of a flat beam of various widths $\alpha = a/R$ in a circular chamber of radius R, as function of position $\eta = x/R$. The hatched area gives the limits of the beam.

a) centred beam, b) off-centred beam.

Figs. 2a and 2b show $\varepsilon_1{}^v$ for beams of different widths across the whole vacuum chamber, for centred and slightly off-centred beams. Even for centred beams, ε_1 is now unequal zero everywhere, but it remains small even for beams filling half the chamber. For off-centred beams, however, ε_1 can become quite large at the beam-edge closest to the wall, and also the tune spread may be increased considerably.

Image Coefficients in Elliptical Chambers

The case of a line charge located at the centre of an elliptical vacuum chamber has been solved by conformal mapping techniques in the classical paper by Laslett [1]. These techniques can still be used for beams situated on the major axis of the ellipse, but we now have to distinguish between beams inside, resp. outside the focal points. For most elliptical chambers, however, the focal points are so close to the walls that we can ignore the latter case here.

As shown in ref. 2), the potential of a line-charge λ located at $x_1 < e$ in an ellipse with half-height h, half-width w, and focal distance $e = \sqrt{w^2 - h^2}$ can be obtained by the three step transformations

$$z' = \arccos\frac{z}{e}$$

$$z'' = \mathrm{sn}\left(\frac{2Kz'}{\pi}, k\right) \quad (2.1)$$

$$z''' = \sqrt{z''^2 - 1} \text{ resp. } \sqrt{z''^2 - 1/k^2}$$

where the first transformation maps the ellipse onto a rectangle, the second one onto a half plane with a gap in the equipotential on the horizontal axis, and the third one closes the gap for auxiliary charges of equal resp. opposite sign at $- x_1$. Averaging over the two cases then yields

$$U = \frac{\lambda}{2\pi\ \varepsilon_o}\ln\left|\frac{\mathrm{dn} + \mathrm{dn}_1}{\mathrm{cn} - \mathrm{cn}_1}\right| \quad (2.2)$$

where cn and dn are Jacobian elliptic functions of argument u (resp. u_1 for subscript 1) with

$$u_{(1)} = \frac{2K}{\pi}\arccos\frac{x_{(1)}}{e} \quad (2.3)$$

$K = K(k)$ is the complete elliptic integral of the first kind, and the modulus k is determined by the transcendental equation

$$\frac{K'}{K} = \frac{2}{\pi}\,\mathrm{Artanh}\,\frac{h}{w} \quad (2.4)$$

$K' = K(k')$ is the elliptic integral of the complementary modulus $k' = \sqrt{1 - k^2}$. It is more convenient, however, to introduce the "nome" q defined by

$$q = \exp(-\ \pi\ K'/K) \quad (2.5)$$

which then is given in terms of the ellipse dimensions by the algebraic equation

$$q = \frac{w - h}{w + h} \quad (2.6)$$

Also computer programs for elliptic functions are usually expressed in terms of the nome, which makes numerical evaluation much easier.

From the potential, we obtain the electric field by differentiation. Subtraction of the direct space charge terms yields the image field component

$$E_x^{IM} = \frac{\lambda}{2\pi\,\varepsilon_0}\left[\frac{2K}{\pi W}\,\frac{\mathrm{cndn}_1}{\mathrm{sn}-\mathrm{sn}_1} - \frac{1}{x-x_1}\right] \qquad (2.7)$$

where $W_{(1)} = \sqrt{e^2 - x_{(1)}^2}$ (2.8)

The image coefficients are obtained from the derivates of the electric field, multiplied by the factor $\pi\,\varepsilon_0\,h^2/\lambda$, and we get for $\varepsilon_1{}^v(x,x_1) = -\,\varepsilon_1{}^h(x,x_1) =$

$$\frac{h^2}{2}\left[\left(\frac{2K}{\pi W}\right)^2 \mathrm{dndn}_1\frac{1-\mathrm{snsn}_1}{(\mathrm{sn}-\mathrm{sn}_1)^2} - \frac{2Kx}{W}\,\frac{\mathrm{cndn}_1}{\mathrm{sn}-\mathrm{sn}_1} - \frac{1}{(x-x_1)^2}\right] \qquad (2.9)$$

where the arguments of the elliptic functions have been changed to

$$u_{(1)} = \frac{2K}{\pi}\arcsin\frac{x_{(1)}}{e} \qquad (2.10)$$

In the limit $x \to x_1$, the expression becomes indeterminate, and we use series development about the beam position to get for $\varepsilon_1{}^v(x_1,x_1) = -\,\varepsilon_1{}^h(x_1,x_1) =$

$$\frac{h^2}{12W_1{}^2}\left[A\left(\frac{2K}{\pi\,\mathrm{cn}_1\mathrm{dn}_1}\right)^2 - \frac{6k'^2\,K\,\mathrm{sn}_1}{\pi\,\mathrm{cn}_1\mathrm{dn}_1}\,\frac{x_1}{W_1} - \frac{4e^2+5x_1{}^2}{2W_1{}^2}\right] \qquad (2.11)$$

where

$$A = (2-k^2) - \tfrac{1}{2}(1+k^2)^2\,\mathrm{sn}_1{}^2 - k^2(1-2k^2)\,\mathrm{sn}_1{}^4 \qquad (2.12)$$

For $x_1 = 0$, we obtain the image coefficient at the centre of the ellipse

$$\varepsilon_1{}^v(0,0) = \frac{h^2}{6e^2}\left[\left(\frac{2K}{\pi}\right)^2 (2-k^2) - 1\right] \qquad (2.13)$$

in agreement with ref. 1). The incoherent image coefficients are shown as function of x_1/h in Fig. 1 for ellipses of various aspect ratios w/h. For beams of finite width, the image coefficients are again obtained from eq. (1.7). A computer program has been written to evaluate the integral, and some results are shown in Figs. 3a and 3b) for centred and slightly off-centred beams for ellipses of an aspect ratio of 3, which corresponds to the ISR vacuum chamber inside magnets.

Image Coefficients in Parallel Plate Geometry

This geometry is mainly of interest for the magnetic images of flat pole pieces. Using image currents of equal sign - rather than charges of opposite sign - and adding the return current at infinity, conformal mapping yields [3] for a beam situated at x_1 in the median plane

$$\varepsilon_2(x,x_1) = \frac{g^2}{2}\left[\frac{1}{(x-x_1)^2} - \frac{\pi^2}{4g^2\,\mathrm{Sinh}^2\,\frac{\pi}{2g}(x-x_1)}\right] \qquad (3.1)$$

where 2g is the pole-piece separation. For a flat beam the integral (1.7) yields

$$\varepsilon_2(\eta;\eta_0,\alpha) = \frac{\tfrac{1}{2}}{(\eta-\eta_0)^2-\alpha^2} - \frac{\pi}{8a}\,\frac{\mathrm{Sinh}\,\pi\,\alpha}{\mathrm{Sinh}^2\,\frac{\pi}{2}(\eta-\eta_0) - \mathrm{Sinh}^2\,\frac{\pi\,\alpha}{2}} \qquad (3.2)$$

This function can be used in the evaluation of the total Q-shift in the ISR.

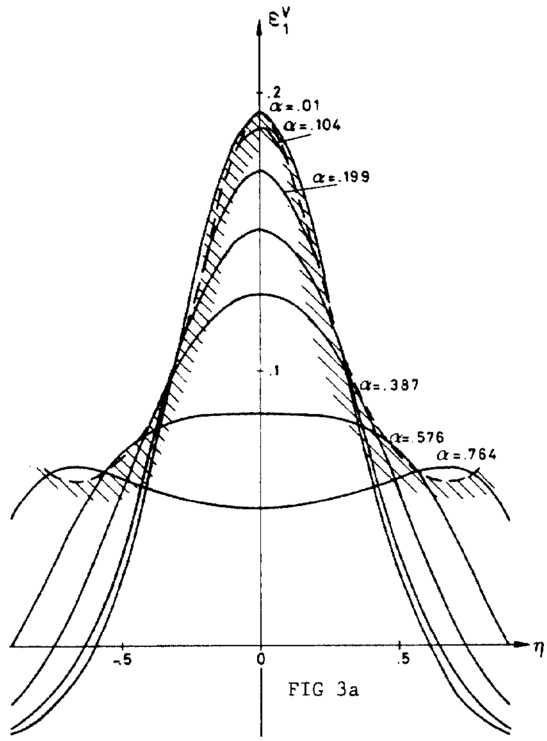

FIG 3a

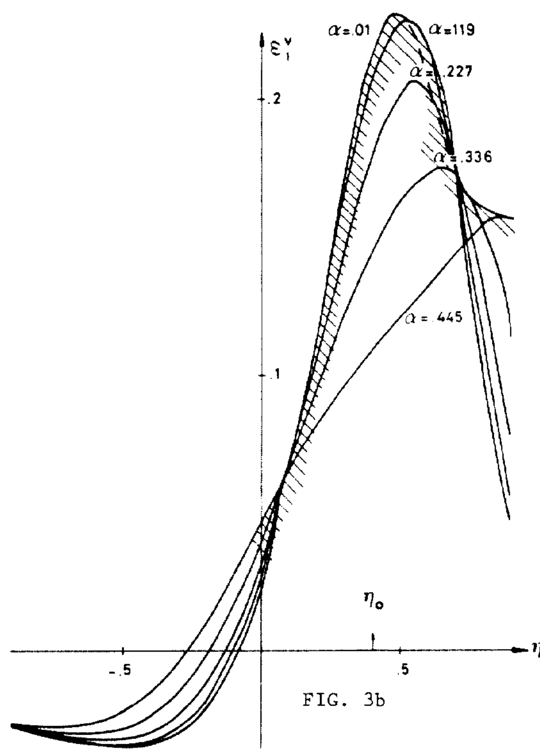

FIG. 3b

Fig. 3 - Incoherent image coefficients of flat beams of various widths α = a/R in an elliptical chamber of aspect ratio w/h = 3, as function of position η = x/R. The hatched area gives the limits of the beam.

a) centred beam, b) off-centred beam.

Direct Space-Charge Coefficients

Analoguous to the image coefficients, we can define the coefficients ε_o^v and ε_o^h due to the direct space-charge force. Since electric and magnetic forces counteract each other, these terms will be multiplied by $1/\gamma^2$ unless a finite neturalization η destroys the balance.

Now we can no longer ignore the vertical extent of the beam, as the coefficients would tend to infinity for vanishing beam dimensions. For a Gaussian beam of standard deviations a and b the horizontal and vertical directions, the potential has been given in integral form by Houssais [4]

$$U(x,y) = \frac{\lambda}{4\pi\,\varepsilon_o}\int_o^\infty \frac{1-\exp\left(-\frac{x^2}{a^2+t}-\frac{b^2}{b^2+t}\right)}{(a^2+t)^{\frac{1}{2}}\,(b^2+t)^{\frac{1}{2}}}\,dt \qquad (4.1)$$

This expression must be differentiated twice under the integral to get the field derivatives, and then the integrals can be evaluated [5] to yield for $y = 0$

$$\varepsilon_o{}^h(x) = \frac{b^2}{\varepsilon^2}\left[\frac{b}{a}\,e^{-\frac{x^2}{a^2}} - 1 + \sqrt{\pi}\,\frac{x}{\varepsilon}\,e^{\frac{x^2}{\varepsilon}}\left(\text{erf}\,\frac{bx}{a\varepsilon} - \text{erf}\,\frac{x}{\varepsilon}\right)\right]$$

$$\varepsilon_o{}^v(x) = \frac{b}{a}\,e^{-\frac{x^2}{a^2}} - \varepsilon_{oh} \qquad (4.2)$$

where $\varepsilon = \sqrt{b^2 - a^2}$. At the beam centre, we get simply

$$\varepsilon_o{}^h(o) = \frac{b^2}{a(a+b)}\,, \quad \varepsilon_o{}^v(o) = \frac{b}{a+b} \qquad (4.3)$$

in agreement with earlier calculations [6] after division by b^2, which factor has been introduced to make the coefficients dimensionless.

We can integrate this expression over a stack in closed form to get

$$\varepsilon_o{}^h = \frac{\sqrt{\pi}}{4}\,\frac{b^2}{a\varepsilon}\left[e^{\left(\frac{x+a}{\varepsilon}\right)^2}\left(\text{erf}\,\frac{b}{\delta}\,\frac{x+a}{\varepsilon} - \text{erf}\,\frac{x+a}{\varepsilon}\right) - e^{\left(\frac{x-a}{\varepsilon}\right)^2}\left(\text{erf}\,\frac{b}{\delta}\,\frac{x-a}{\varepsilon} - \text{erf}\,\frac{x-a}{\varepsilon}\right)\right] \qquad (4.4)$$

$$\varepsilon_o{}^v = -\varepsilon_{oh} + \frac{\sqrt{\pi}}{4}\,\frac{b}{a}\left(\text{erf}\,\frac{x+a}{\delta} - \text{erf}\,\frac{x-a}{\delta}\right)$$

$$\varepsilon = \sqrt{b^2 - \delta^2}$$

where we have replaced a by δ - the tail half-width - and used a for the stack half-width as before. Inside the beam, Poisson's equation must hold, and the density profile over the stack is given by $\frac{\lambda}{\pi\, b^2}$ times the sum of the two coefficients.

At the beam centre, we now get

$$\varepsilon_o{}^h(o) = \frac{\sqrt{\pi}}{2}\,\frac{b^2}{a\varepsilon}\;e^{\frac{a^2}{\varepsilon^2}}\left(\text{erf}\,\frac{ba}{\delta\varepsilon} - \text{erf}\,\frac{a}{\varepsilon}\right)$$

$$\varepsilon_o{}^v(o) = -\varepsilon_{oh} + \frac{\sqrt{\pi}}{2}\,\text{erf}\,\frac{a}{\delta} \qquad (4.5)$$

In the limit of vanishing tails - corresponding to a horizontally uniform beam - these expressions become

$$\varepsilon_o{}^h(o) = \frac{\sqrt{\pi}}{2}\,\frac{b}{a}\,w\!\left(i\,\frac{a}{b}\right)$$

$$\varepsilon_o{}^v(o) = \frac{\sqrt{\pi}}{2}\,\frac{b}{a}\left[1 - w\!\left(\frac{ia}{b}\right)\right] \qquad (4.6)$$

where $w(x)$ is the complex error function. At the beam edge, $\varepsilon_o{}^h$ changes suddenly to a negative value, while $\varepsilon_o{}^v$ is continuous

$$\varepsilon_o{}^h(a) = \frac{\sqrt{\pi}}{4}\,\frac{b}{a}\left[w\!\left(i\,\frac{2a}{b}\right) \pm 1\right]$$

$$\varepsilon_o{}^v(a) = \frac{\sqrt{\pi}}{4}\,\frac{b}{a}\left[1 - w\!\left(i\,\frac{2a}{b}\right)\right] \qquad (4.7)$$

These coefficients are shown in Fig. 4 for stacks of various tail-widths.

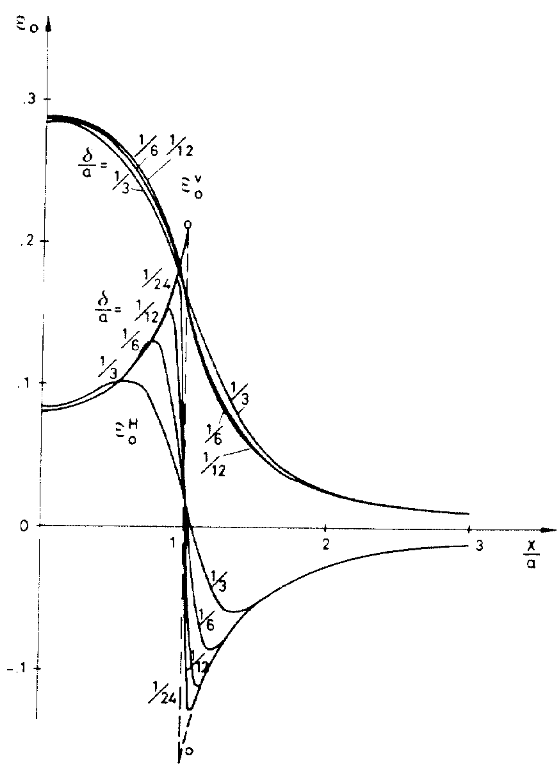

Fig. 4 - Direct space-charge coefficient for a stacked beam of height-to-width ratio $b/a = 5/12$, and various flank-widths δ/a.

Incoherent Q-Shift of Stacked Beam

The geometric coefficients calculated in the previous sections can now be used to calculate the Q-shifts of stacked beams in storage rings. For a machine consisting partially of circular, and partially of elliptic vacuum chamber as the ISR, the incoherent Q-shifts in the two planes are given by $\Delta Q =$

$$\frac{N\, r_0\, \bar{\beta}}{\pi\, \beta^2\, \gamma}\left(c_1 \frac{\varepsilon_1^{\,circ}}{R^2} + c_2 \frac{\varepsilon_2^{\,ell}}{h^2} + c_3\, \beta^2 \frac{\varepsilon_2^{\,pp}}{g^2} + \frac{\varepsilon_0}{\gamma^2\, b^2}\right)$$

with N – total number of particles
r_0 – classical proton radius
$\bar{\beta}$ – average beta function
β,γ – beam velocity/energy
η – neutralization
c_i – circumference factors
ε_i – geometric coefficients

This still neglects the influence of bellows, pick-up and clearing electrodes, resonant tanks, and other cross-section variations. Nevertheless, agreement with experimentally measured values is quite satisfactory, as can be seen in Fig. 5, which shows the Q-shifts in the centre of five 3 A sub-stacks of 6 mm half-width, with centres moving from + 39 mm to − 9 mm corresponding to stacking on the 8C working line in the ISR.

Conclusions

The incoherent image coefficients of thin beams in elliptic chambers have been expressed in closed form, and are summarized in two graphs, including the limiting cases of circular and parallel plate geometries. Several cases of beams of finite widths are also shown graphically, as well as the contribution due to direct space-charge.

For circular chambers, which are usually proposed for future superconducting machines, it can be seen that the image coefficients can become quite large for excentric beams, and should not be neglected. As an example, the geometric coefficients are used to calculate the tune shifts of substacks on a dynamically compensated working-line in the ISR, and show better agreement with experiment than had been expected for the idealized geometry.

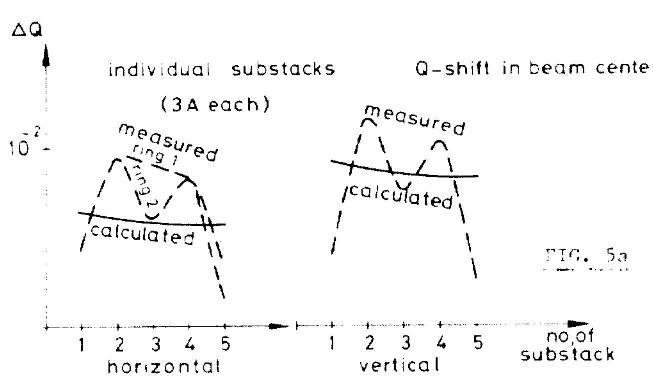

FIG. 5a

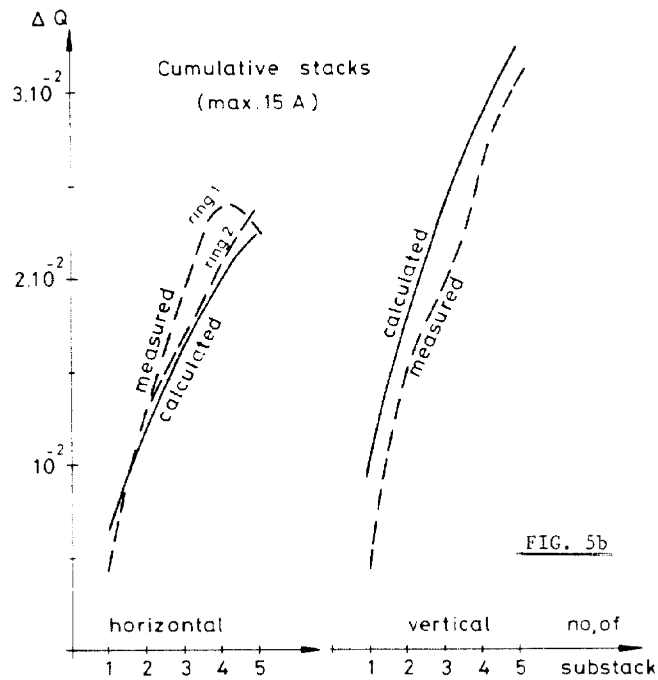

FIG. 5b

Fig. 5 – Q-shift of 3 A substack on the ISR working-line 8C. a) individual, b) cumulative.

References

1) L.J. Laslett; On intensity limitations imposed by transverse space-charge effects in circular particle accelerators. Proc. Brookhaven Summer Study 1963 (BNL 7534).

2) B. Zotter; Image fields of an off-centre particle beam in an elliptic vacuum chamber. CERN/ISR-TH/74-11 (1974).

3) B. Zotter; Incoherent Q-shift of a flat, off-centred particle beam in an elliptic chamber. CERN/ISR-TH/74-38 (1974).

4) B. Houssais; Thesis Univ. Rennes (1967).

5) B. Zotter; Q-shift due to the direct space-charge field of stacked particle beams. CERN/ISR-TH/75-5 (1975).

6) L. Teng; Transverse space-charge effects. ANLAD-59 (1963).